Two Photon Physics at LEP

Valery P. Andreev[a]
e-mail: Valeri.Andreev@cern.ch

[a]Department of Physics and Astronomy,
202 Nicholson Hall,
Louisiana State University,
Baton Rouge, LA 70803, USA

A review of the experimental results on two photon collisions at LEP is given. The total cross section for $\gamma\gamma \rightarrow hadrons$ is measured for two-photon centre-of-mass energies up to 145 GeV. The QCD predictions are tested with measurements of the cross section for deep inelastic electron photon scattering (in terms of photon structure function), of total hadronic cross section for virtual $\gamma^*\gamma^*$ collisions, and in collisions of quasi-real photons with jet, inclusive particle and heavy flavour ($c\bar{c}$ and $b\bar{b}$) production. Resonance formation in $\gamma\gamma$ collisions and its connection to glueball searches is also discussed.

1. Introduction

A quasi-real photon interacts as a hadron due to quantum fluctuations into vector mesons or into quark-antiquark pairs. The $\gamma\gamma$ cross section is composed (Figure 1) by a "soft (VDM)" interaction, which can be described by hadronic phenomenology, like the Regge poles, a point like two-photon reaction, $\gamma\gamma \rightarrow q\bar{q}$, which is exactly calculable in QED (direct component) and a "hard component" (resolved or anomalous or QCD component) which implies the knowledge of the quark and gluon density in the photon. The "hard component" of two-photon interactions can be accessed in measurements of high-p_t single particle and jet production, the heavy flavour production and scattering of highly virtual photons. Then a hard physical scale is given by p_t or by c(b)-quark mass or by large virtuality Q^2 of the photon. Resonance formation in two-photon collisions is an important tool for resolving a glueball observation puzzle. The LEP e^+e^- collider is an ideal place to study two photon physics. The background from the annihilation events is normally very low, especially at LEP2 energies ($\sqrt{s} > 160$ GeV).

2. Total hadronic $\gamma\gamma$ cross section

The cross section of $\gamma\gamma \rightarrow hadrons$ process has been measured at LEP by the L3 [1,3] and the OPAL [2] for $\gamma\gamma$ centre-of-mass energies up to 145 GeV. The energy of a photon-photon collision is determined from the hadronic final state. The visible mass, $\mathrm{W_{vis}}$, of the event is calculated from the four-momentum vectors of the measured particles (tracks and calorimetric clusters). The hadronic final state is not always fully contained in a detector acceptance. Unfolding procedure is applied to go from the measured $\mathrm{W_{vis}}$ to the true $\gamma\gamma$ centre-of-mass energy $\mathrm{W}_{\gamma\gamma}$. From the number of events, corrected with Monte Carlo generator (PYTHIA or PHOJET) in each $W_{\gamma\gamma}$ bin, the cross section $d\sigma(e^+e^- \rightarrow e^+e^- hadrons)$ is measured, Figure 2(left). From the $d\sigma(e^+e^- \rightarrow e^+e^- hadrons)$ the total cross section of two real photons is extracted by calculating the photon flux and extrapolating the hadronic two-photon processes to zero Q^2.

Figure 2(right) shows the $\sigma_{\gamma\gamma}$ measurements by L3 and OPAL collaborations. The difference between the open and the full dots reflects the difference on selection efficiency and unfolding corrections given by the two generators. The measurements by L3 and OPAL agree when the same generator is used in the analysis, but there is a

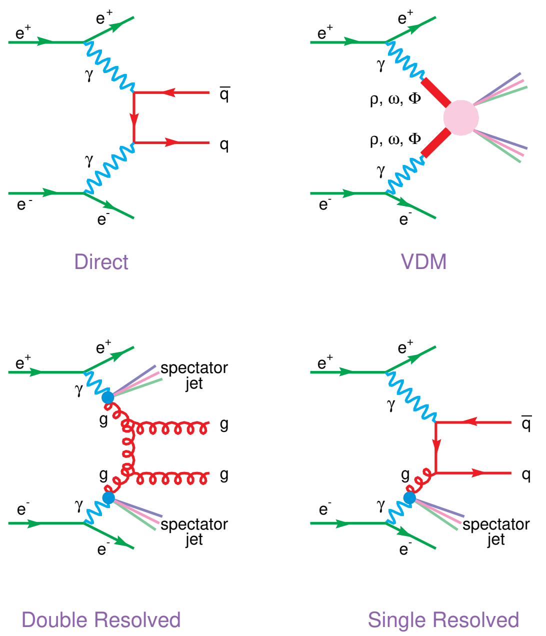

Figure 1. Hadronic final state in two-photon collisions.

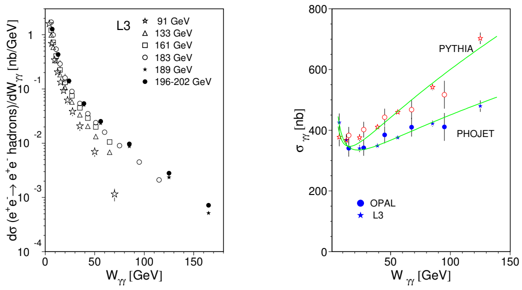

Figure 2. Total cross section for hadron production in two-photon collisions. (left) The cross section $d\sigma(e^+e^- \to e^+e^- hadrons)/dW_{\gamma\gamma}$ measured at various LEP beam energies, 91 GeV $< \sqrt{s} <$ 202 GeV. (right) The two-photon total cross section obtained by correcting the full data sample with PYTHIA and PHOJET. The Regge fits described in the text are superimposed to the data.

systematic difference of $\simeq$ 20% between the two Monte Carlo models used in analysis. This is mostly due to a different modelling of diffractive events. Discrepancy between data and predictions in a diffractive region is demonstrated by OPAL by measuring the maximum rapidity gap $\Delta\eta_{max}$, Figure 3. It shows that PYTHIA and PHOJET both underestimate the particle production in the diffractive region (high values of $\Delta\eta_{max}$). Finally, the cross section is given as average of the two generators, Figure 4, where a model dependence is dominating systematic error.

A parametrisation by A. Donnachie and P.V. Landshoff [4] of the form $\sigma_{\rm tot} = A\, s^{\epsilon} + B\, s^{-\eta}$ describes well the energy behaviour of all total hadron-hadron cross sections. A fit with A, B and ϵ as free parameters ($\eta = 0.34 \pm 0.02$[5]) gives:
$\epsilon = 0.250 \pm 0.016$, L3
$\epsilon = 0.101 + 0.025/-0.019$, OPAL
The L3 ϵ value is about a factor of 2.5 higher than the universal value $\epsilon = 0.095 \pm 0.02$ [5], independent on the Monte Carlo model used to correct the data, while OPAL fit is consistent with PDG value. The L3 fit [3] shows that reggeon part (slope described by η) and Pomeron part (slope described by ϵ) of the fit are strongly correlated. Fitting only high energy part (Pomeron) the slope increases from $\epsilon = 0.089 \pm 0.005$ to $\epsilon = 0.183 \pm 0.014$ for $W_{\gamma\gamma}^{min}$ from 17 GeV to 47 GeV. It means that the slope is not a fundamental constant but rather illustrates the inset of QCD phenomena.

The two-photon cross section at high energies can be estimated from proton-proton and photoproduction total cross sections assuming factorization for the Pomeron term: $\sigma_{\gamma\gamma} \approx \sigma_{\gamma\rm p}^2/\sigma_{\rm pp}$. The predictions thus obtained are consistent with the two-photon measurement, Dual Parton Model curve [8] in Figure 4(left). Several QCD inspired models [6,7,9,10] are also in a qualitative agreement with the data (Figure 4).

3. Charm and beauty production

The production of heavy quarks in two-photon collisions consists mainly of charm quarks. Because of their smaller electric charge and larger mass, the production of b-quarks is expected to be suppressed by more than two orders of magnitude relative to the production of charm quarks.

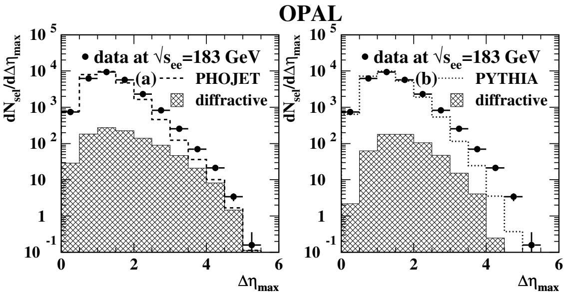

Figure 3. Maximum rapidity gap $\Delta\eta_{max}$ distribution. The gap $\Delta\eta$ is the difference of the pseudo-rapidity η of any two particles, neutral or charged. Both PYTHIA and PHOJET underestimate the particle production in the diffractive region (high values of $\Delta\eta_{max}$).

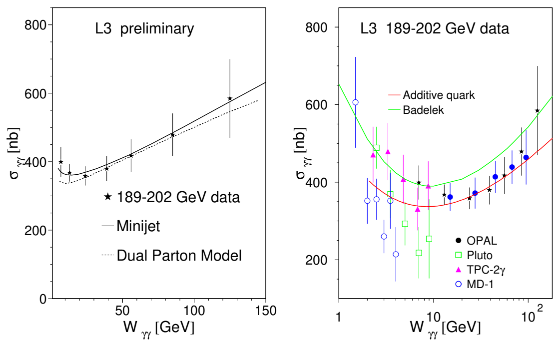

Figure 4. Predictions for two-photon total cross section [8–10].

The resolved photon cross section is dominated by the photon-gluon fusion diagram $\gamma g \to c\bar{c}, b\bar{b}$. At LEP energies, the direct and resolved processes are predicted to give comparable contributions to the cross section [12]. Measurements of charm production in two-photon collisions were done at LEP by ALEPH[13], L3[14] and OPAL[16] collaborations. Beauty production has been measured by L3[15] for the first time in gamma-gamma collisions.

3.1. Charm production

Charm particles in the final state were identified by the reconstruction of charged D^* mesons decays by ALEPH, L3 and OPAL. Both charm and beauty quarks were identified by the L3 collaboration using tagging by electrons and muons from semileptonic charm and beauty decays. ALEPH has also used muon tag for charm measurement. OPAL collaboration measured the direct and single-resolved charm cross sections separately. The scaled D^* transverse momentum $x_t^{D^*}$ which is the ratio of $P_t^{D^*}$ to $W_{vis}/2$ is sensitive to the ratio of the direct and the single-resolved process. The fit to the OPAL D^* data gives about 1:1 for the ratio in the data, which translates into the direct process contribution to the total cross section to be (401 ± 124) pb and the single-resolved contribution to be (562 ± 202) pb. The total inclusive charm cross sections are plotted in Figure 5 together with previous measurements. The data are compared to the theory predictions of Ref.[12]. The dashed line corresponds to the direct process, NLO QCD calculation, while the solid line shows the QCD prediction for the sum of the direct and the resolved processes calculated to NLO accuracy. The cross section of charm production with a D^* tag is in agreement with the lepton tag measurement.

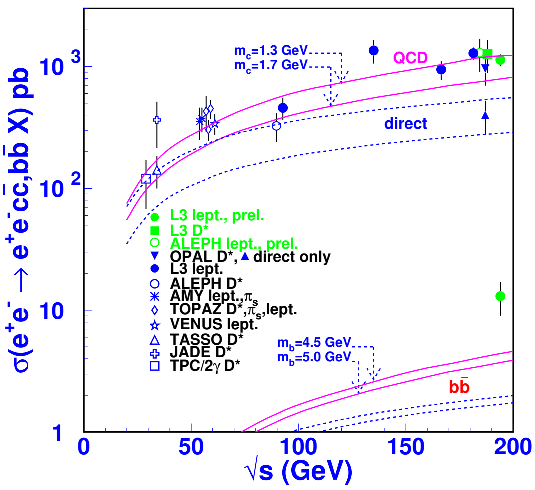

Figure 5. Charm and beauty production in two-photon collisions.

In Figure 6 the L3 and OPAL measurements of the differential cross section $d\sigma/dP_T^{D^*}$ are compared to NLO QCD calculations by Binnewies et al. [21] using the massless approach and by Frixione et al. [22] using the massive approach. The two measurements are in agreement with each other and with both QCD calculations at high transverse momenta. At low P_T the massive approach underestimates the data.

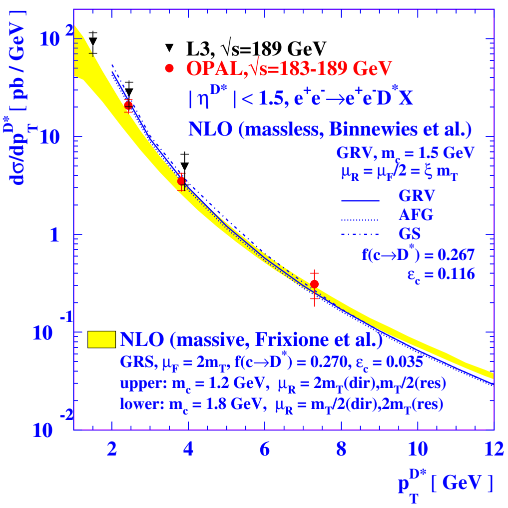

Figure 6. The differential D^* cross section $d\sigma/dP_T^{D^*}$ by L3 and OPAL.

The L3 collaboration measured the cross sections $\sigma(e^+e^- \to e^+e^-c\bar{c}X)$ and $\sigma(\gamma\gamma \to c\bar{c}X)$ in the interval 5 GeV $\leq W_{\gamma\gamma} \leq$ 70 GeV. Figure 7 shows the preliminary $\sigma(\gamma\gamma \to c\bar{c}X)$ as function of $W_{\gamma\gamma}$ at $\sqrt{s} = 189-202$ GeV. The continuous line is the fit by parametrization $\sigma_{\rm tot} = A\,s^\epsilon + B\,s^{-\eta}$, with fixed value of $\eta = -0.34$ [5]. The dashed curve shows the expectation from the PYTHIA leading order Monte Carlo. The expected slope is smaller than the slope observed in the data. The dotted curve is the measured by L3 total cross section $\sigma(\gamma\gamma \to \text{hadrons})$ [3] scaled by factor 1/20. The fit gives for the Pomeron slope $\epsilon = 0.400 \pm 0.062$(stat). A steeper rise with energy is observed as compared to hadron-hadron cross sections and to $\sigma(\gamma\gamma \to hadrons)$.

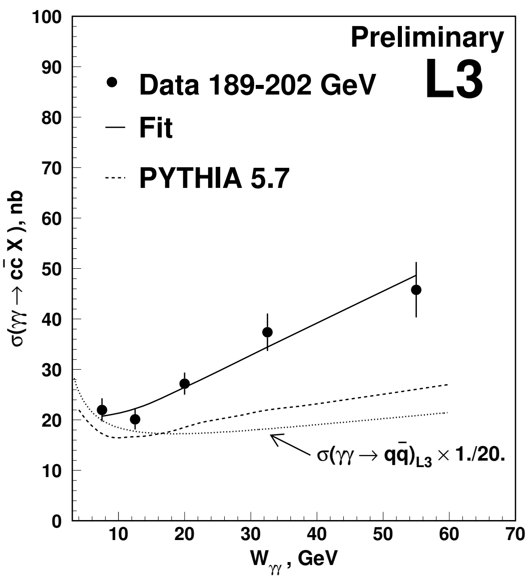

Figure 7. Cross section $\sigma(\gamma\gamma \to c\bar{c})$ versus $W_{\gamma\gamma}$ by L3.

Using a sample of single-tagged events OPAL measured $F_{2,c}^{\gamma}$ photon structure function at $\langle Q^2\rangle = 20$ GeV^2, Figure 8. Vermaseren (direct only process) and HERWIG Monte Carlo event generators have been used in the study. Within limited statistics of 30 ± 6 D^* mesons in events, where one beam electron is scattered into detector, both Monte Carlo generators are in agreement with the data distributions. The data suggest nevertheless a cross-section which is above the purely point-like component, i.e. the hadron-like component of $F_{2,c}^{\gamma}$ is non-zero.

3.2. Beauty production

Leptons from b semi-leptonic decays are more energetic than from charm semi-leptonic decays and non-charm two-photon processes. To select $b\bar{b}$ events L3 apply cuts on the lepton momentum and transverse momentum with respect to the closest jet defined by excluding the lepton from

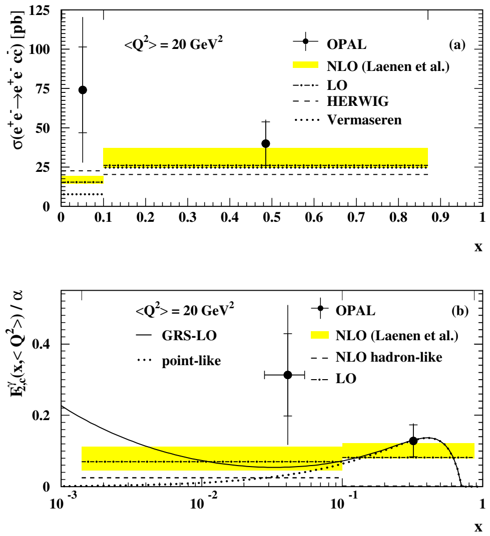

Figure 8. The $\sigma(\mathrm{e}^+\mathrm{e}^- \to \mathrm{e}^+\mathrm{e}^-\mathrm{c}\bar{\mathrm{c}}\mathrm{X})$ and $F_{2,c}^{\gamma}$ at $\langle Q^2 \rangle$ =20 GeV^2 by OPAL.

the jet. After all cuts are applied 103 electron and 125 muon candidates remain. The beauty purity is 51.0 %. The beauty selection efficiency is about 1.0 %. The preliminary beauty production cross section in $\gamma\gamma$ collisions has been measured to be $\sigma^{ee\to eebbX} = 13.0 \pm 1.8$ (st) ± 3.6 (sys) pb.

The measured b cross section lie about 4 standard deviations above QCD prediction, Figure 5. This is particularly interesting as measurements of beauty production in p$\bar{\mathrm{p}}$ collisions by CDF [17] and DØ [18] as well as in ep collisions by H1 [19] and ZEUS [20] have been found to be a factor ∼2–3 higher than NLO QCD predictions.

4. Electron Photon Deep Inelastic Scattering

The photon structure function is measured via the interaction of two virtual photons $e^+e^- \to e^+e^-\gamma^*\gamma \to e^+e^-$hadrons. The photon ($\gamma^*$) of high virtuality Q^2 is used as a probe for the structure of the quasi-real target photon (γ) with virtuality $P^2 \sim$0 (single-tag events). The cross section as function of dimensionless deep inelastic scattering variable x and Q^2 is proportional to the structure function $F_2^\gamma(x, Q^2)$. Figure 9 illustrates the composition of the $F_2^\gamma(x, Q^2)$ versus x. Single-tag events were studied by all four LEP collaborations [23–27]. The compilation [28] of results for F_2^γ as function of x for fixed Q^2 is shown in Figure 10 and as function of Q^2 for different x intervals is shown in Figure 11. As one can see the Quark Parton Model is not sufficient to describe data at low x. The data do not show a strong rise of the photon structure function at very low x, this is to compare with HERA experiments measurement of rise of the proton structure function. The measured F_2^γ shows clearly a linear growth with $\ln Q^2$ as expected by QCD.

The structure function for double tag case was firstly measured by the PLUTO collaboration[29]. The L3 collaboration for the first time since PLUTO measured the structure function of the virtual photon [26]. The measured with double-tag events an effective structure function at $Q^2 = 120$GeV^2 and $P^2 = 3.7$GeV^2 is plotted in Figure 12. The value is higher than predicted by the QPM, but still compatible within the combined statistical and systematic uncertainties.

The LEP Working Group for Two Photon Physics has undertaken an effort to understand the systematics for the photon structure function measurements. Several distributions were studied [31], namely, the reconstructed hadronic mass, the transverse energy, the number of tracks, the transverse momenta of tracks and the hadronic energy flow as a function of the pseudorapidity. It was found that the results of different experiments are closer to each other than the sizable differences observed between the data and the model (HERWIG and PHOJET).

The analyses of the leptonic structure function show the importance of non-zero virtuality of the target photon and the importance of the interference terms in the cross section decomposition [30]. The latest review on the photon structure is given in Ref. [32].

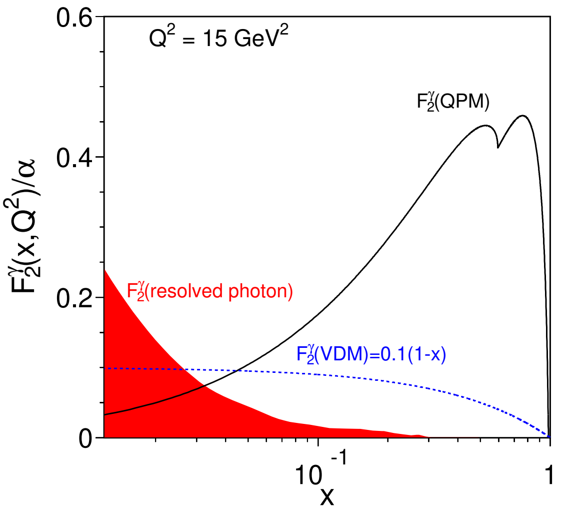

Figure 9. Contributions to the hadronic structure function F_2^γ.

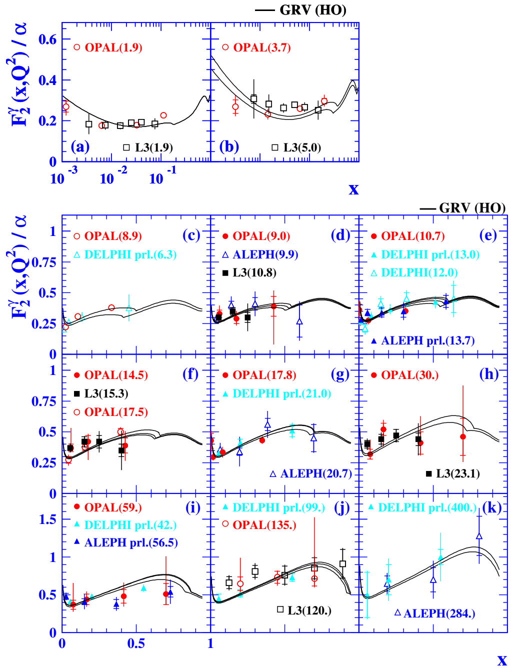

Figure 10. F_2^γ as function of x for different Q^2.

5. Total hadronic $\gamma^*\gamma^*$ cross section

The cross-section measurement for scattering of two virtual photons is considered as "golden" process to test the BFKL dynamics which is proposed in [33]. Double-tag events in two-photon collisions are studied by the L3 collaboration at the LEP center of mass energies $\sqrt{s} \simeq 91 - 202$ GeV. The cross-section of $\gamma^*\gamma^*$ collisions is measured at an average photon virtuality up to $\langle Q^2 \rangle = 15$ GeV^2. The $\gamma^*\gamma^*$ interaction can be seen as the interaction of two $q\bar{q}$ pairs scattering off each other via multiple gluon exchange. For the highly virtual two-photon process, with $Q_1^2 \simeq Q_2^2$, the calculation can be verified without phenomenological inputs as non-perturbative QCD contributions are expected to vanish [35]. In this scheme the cross-section for the collision of two virtual photons is $\sigma_{\gamma^*\gamma^*} \approx \frac{\sigma_0}{\sqrt{Q_1^2 Q_2^2 Y}} \left(\frac{W_{\gamma^*\gamma^*}}{\sqrt{Q_1^2 Q_2^2}}\right)^{\alpha_P - 1}$, where α_P is the "hard Pomeron" intercept.

The L3 selects [34] 137 events at $\sqrt{s} \simeq 91$ GeV with $\langle Q^2 \rangle = 3.5$ GeV^2, 34 events at $\sqrt{s} \simeq 183$ GeV with $\langle Q^2 \rangle = 14$ GeV^2 and 324 events at $\sqrt{s} \simeq 189 - 202$ GeV with $\langle Q^2 \rangle = 15$ GeV^2. The dominant background processes are $e^+e^- \rightarrow e^+e^-\tau^+\tau^-$ and misidentified single-tagged events.

In Figure 13 the measured cross section $e^+e^- \rightarrow e^+e^-\gamma^*\gamma^* \rightarrow e^+e^- hadrons$ is plotted together with prediction for direct (QPM) process and with the prediction of QCD Monte Carlo model implemented in PHOJET generator of R. Engel [8]. The cross section is plotted as function of variable $Y = ln(s/s_0) \simeq ln(W_{\gamma^*\gamma^*}/Q_1 Q_2)$. The QPM cross section lies below the data, while QCD prediction is in a reasonable agreement with the data. The value of the cross section at $5 < Y < 7$ exceeds the Monte Carlo prediction by about 3.5 standard deviations.

The two-photon cross-section is extracted from the $e^+e^- \rightarrow e^+e^-$hadrons cross-section, σ_{ee}, by using only the transverse photon luminosity function [36], $\sigma_{\rm ee} = L_{TT} \cdot \sigma_{\gamma^*\gamma^*}$. The two-photon cross-section, $\sigma_{\gamma^*\gamma^*}$, after subtraction of the QPM contribution is shown in Figure 14 as a function of Y. The predictions of the one-gluon ex-

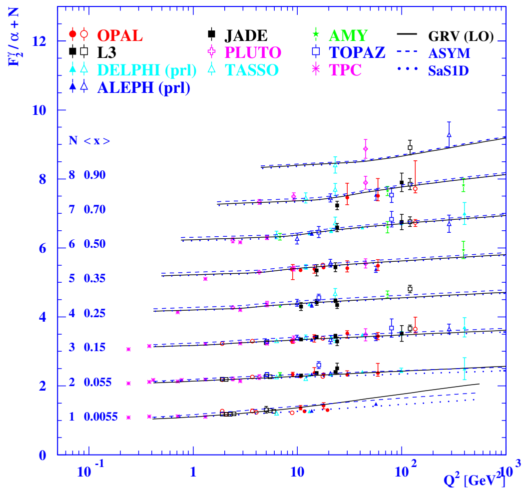

Figure 11. The Q^2 evolution of the hadronic structure function F_2^γ.

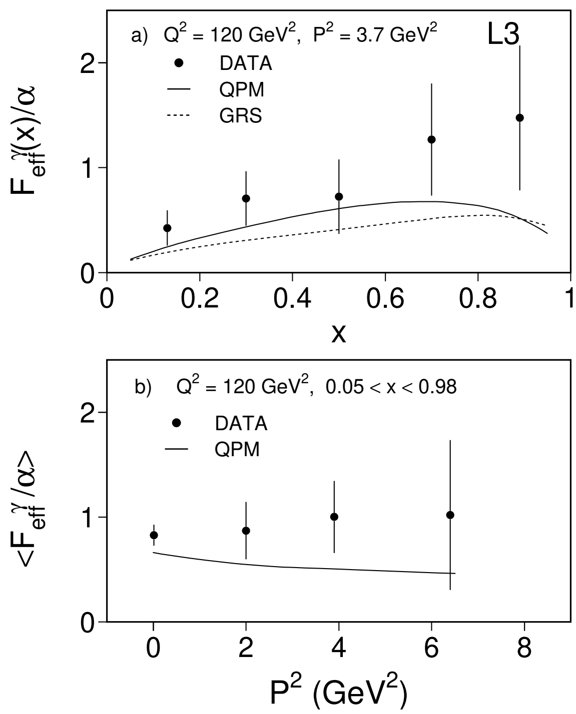

Figure 12. $F^\gamma_{\text{effective}}$ in double-tag events by L3. a) F^γ_{eff}/α for virtual photons, compared with the QPM and the QCD calculation. The QCD calculation considers only transverse photons; therefore it is not really comparable with the double-tag data. b) Dependence on P^2 of F^γ_{eff}/α averaged over $x = 0.05 - 0.98$ for single-tag and double-tag data, compared with the QPM prediction.

change diagram and the LO BFKL are also shown in Figure 14. The one-gluon exchange prediction is below the data. The LO BFKL expectation is too high. By leaving α_P as a free parameter, a fit to the three sets of data, yields $\alpha_P - 1 = 0.33 \pm 0.02$, $\chi^2/dof = 4.0/9$ which is smaller than expected from the LO BFKL calculations ($\alpha_P - 1 = 0.53$). The fit result is shown in Figure 14 as a continuous line.

6. Jet and single particle production

Di-jet production, the production of charged hadrons and K^0_S mesons in the collisions of quasi-real photons has been measured by OPAL [37]. The production of π_0 and K^0_S mesons has been measured by L3 in [40,41].

The inclusive two-jet cross section is shown in Figure 15a as a function of E_T^{jet}. The distribution is compared to a NLO QCD calculation [38]. The measured cross sections are in good agreement with NLO QCD calculations except for the first bin were the NLO calculations are not reliable. The inclusive two-jet cross section is dominated by the resolved processes in the low E_T^{jet} region, at high E_T^{jet} the direct process contribution is the largest. The Monte Carlo models PYTHIA and PHOJET describe the transverse energy flow around the jets reasonably well.

Figure 15b shows the inclusive p_T distribution for the charged hadrons measured in $\gamma\gamma$ interactions by OPAL and compared to the p_T distribution measured in γp and hp ($h = \pi, K$) interactions by WA69. There is an evidence for hard photon interactions (direct process contribution) in addition to the hadronic photon interactions. A clear deviation is seen at large p_T from the exponential fall-off expected for purely hadronic

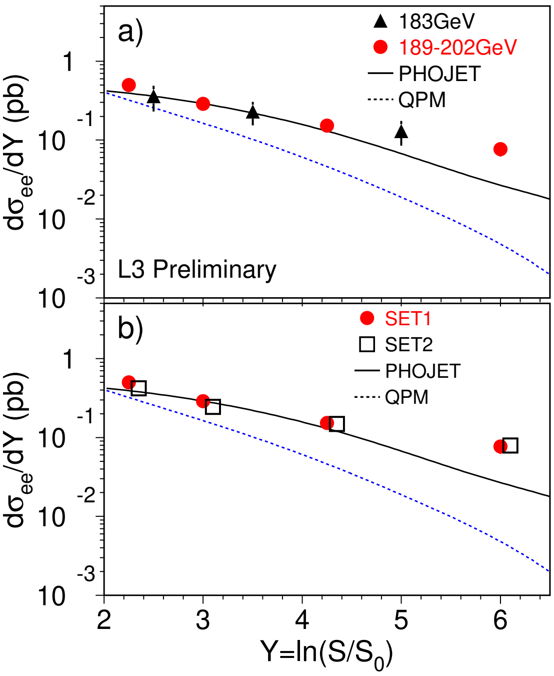

Figure 13. Cross section for $ee \to eeq\bar{q}$ in double-tag events by L3.

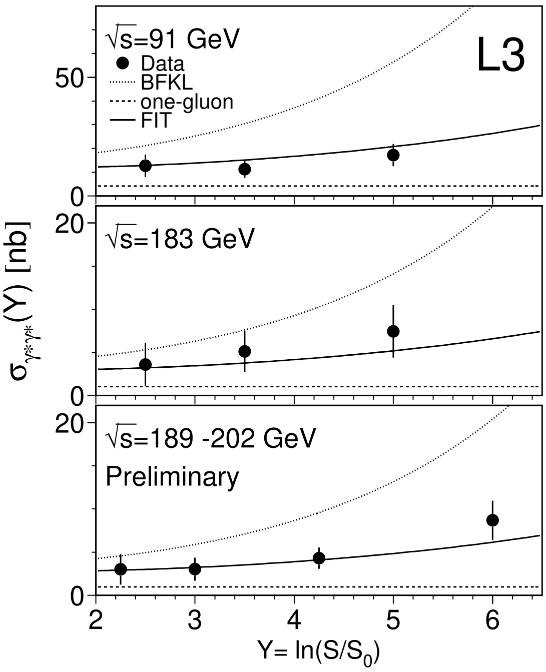

Figure 14. Two-photon cross-section for $\gamma^*\gamma^* \to q\bar{q}$ after subtraction of the QPM contribution.

interactions.

Figure 16 shows the inclusive p_T distribution for π_0 and K_S^0 mesons measured by L3 and compared to NLO QCD calculations [38] The transverse momentum and pseudorapidity distributions of the K_S^0 mesons are well reproduced by the NLO calculations, while high p_T part of the π_0 spectrum is in excess of the prediction. Both π_0 and K_S^0 mesons spectra are significantly underestimated by the Monte Carlo models PYTHIA and PHOJET.

7. Resonance formation in two-photon collisions at LEP

Resonance formation in two-photon collisions has a particular interest due to connection to glueball and exotic (hybrid, four quark) state searches. Since gluons do not couple directly to photons, the two-photon width of a glueball is expected to be very small. A state that can be formed in a gluon rich environment but not in two-photon fusion has the typical signature of a glueball. According to lattice QCD predictions [51], the ground state glueball has J^{PC}= 0^{++} and a mass between 1400 and 1800 MeV. The 2^{++} tensor glueball is expected in the mass region around 2200 MeV.

At LEP resonances are studied mostly by L3 $(\eta', a_2, a_2', f_2', \eta(1440), f_1(1420), \eta(1295), f_J(1750), \eta_c, \chi_{c2}, \eta_c')$ [39,44,45,43]. The χ_{c2} has been also measured by OPAL [46], search for η_c' has been also performed by DELPHI [47] and search for $f_0(1500)$ and $f_J(1710)$ was done by ALEPH [48].

The upper limit of 1.4 eV at 95% CL was obtained by L3 for the $\xi(2230)$ production in the K$_S^0$K$_S^0$ decay channel [42] under the hypothesis of a pure spin-two helicity-two contribution. The BES Collaboration confirmed the observation by the Mark III Collaboration of a resonance, the $\xi(2230)$ [52], produced in radiative decays of the J/ψ particle (gluon rich environment). All this

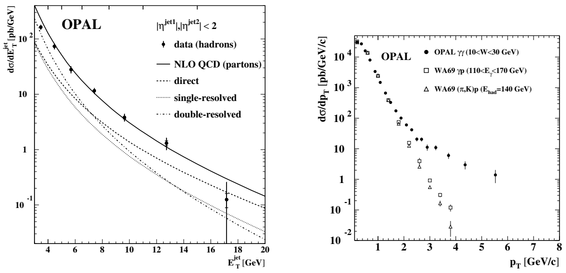

(a) (b)

Figure 15. (a) The inclusive two-jet cross section as a function of E_T^{jet} by OPAL compared with the NLO QCD calculations [38], (b) the charge hadron p_T distribution measured in $\gamma\gamma$ interactions is compared to the p_T distribution measured in γp and hp $(h = \pi, K)$ interactions.

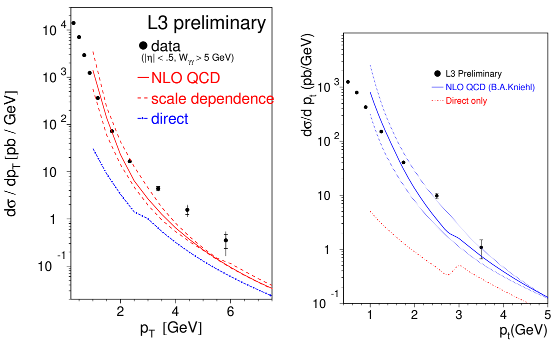

Figure 16. The inclusive π_0 (left) and K_S^0 (right) differential cross sections measured by L3, compared with NLO QCD calculations [38].

gives a strong support to the interpretation of this resonance as a glueball state.

Production of the glueball candidates $f_0(1500)$ and $f_J(1710)$ in $\gamma\gamma$ collisions has been studied by ALEPH via decay to $\pi^+\pi^-$. No signal from either resonance is seen, and the upper limits on the product of two-photon width and $\pi^+\pi^-$ branching ratio have been calculated to be 0.31 keV and 0.55 keV at 95 % CL, respectively.

Formation of light resonances in $\mathrm{K_S^0\,K^\pm\pi^\mp}$ and $\eta\,\pi^+\pi^-$ final states in $\gamma\gamma$ collisions at LEP has been done by L3 in [43]. The mass spectrum

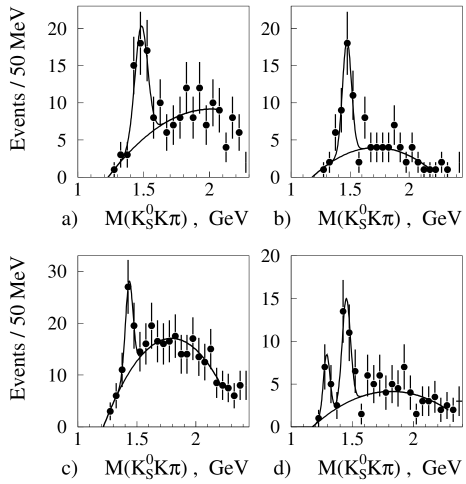

Figure 17. $\mathrm{K_S^0\,K^\pm\pi^\mp}$ spectra for different $\mathrm{P_T^2}$ bins by L3. a) $\mathrm{P_T^2} < 0.02\mathrm{GeV}^2$, b) $0.02 < \mathrm{P_T^2} < 0.2\mathrm{GeV}^2$, c) $0.2 < \mathrm{P_T^2} < 1.\mathrm{GeV}^2$ and d) $1. < \mathrm{P_T^2} < 7.\mathrm{GeV}^2$. In the highest $\mathrm{P_T^2}$ bin, (d), also the peak of the $\mathrm{f_1(1285)}$ is present.

of the $\mathrm{K_S^0\,K^\pm\pi^\mp}$ final state shows an enhancement around 1470 MeV, which is identified with the pseudoscalar meson $\eta\,(1440)$. This state is observed in untagged $\gamma\gamma$ collisions for the first time and the value of its two–photon width is found to be $\Gamma_{\gamma\gamma}(\eta\,(1440))\cdot\mathrm{BR}(\eta\,(1440)\rightarrow\mathrm{K\bar{K}}\pi) = 0.212 \pm 0.05\mathrm{stat} \pm 0.015\mathrm{sys}$ keV. In order to separate $\eta\,(1440)$ and $\mathrm{f_1(1420)}$ contributions, the data were subdivided in four $\mathrm{P_T^2}$ bins (Figure 17). It was noticed that $\mathrm{P_T^2} \simeq \mathrm{Q^2}$, where $\mathrm{Q^2}$ is the maximum virtuality of the two photons. In the highest $\mathrm{P_T^2}$ bin, $1 < \mathrm{P_T^2} < 7\mathrm{GeV}^2$, also the $\mathrm{f_1(1285)}$ is present. Clear evidence is obtained for the formation of the axial vector mesons $\mathrm{f_1(1420)}$ and $\mathrm{f_1(1285)}$. In the $\eta\,\pi^+\pi^-$ channel only the $\mathrm{f_1(1285)}$ is observed and upper limits for the formation of $\eta\,(1440)$ and $\eta\,(1295)$ are given which are stronger than the ones established by Crystal Ball collaboration [53]. The analysis shows that $\eta(1440)$ may have large gluon admixture.

The two-photon width of η_c from two-photon formation measurements is in agreement with the value measured in $p\bar{p} \rightarrow \gamma\gamma$ annihilation, while for χ_{c2} there is discrepancy. The combined two-photon result [45,46,49,50] is $\Gamma_{\gamma\gamma}(\chi_{c2}) = 1.23 \pm 0.23$ keV to compare with the latest E835 [54] $\Gamma_{\gamma\gamma}(\chi_{c2}) = 0.31 \pm 0.05 \pm 0.04$ keV, which confirms the previous E760 measurement [55]. The measured by L3 η_c form-factor is compatible with J/Ψ pole and is in agreement with calculations of ref. [56].

No η_c' signal is observed at LEP [44,47].

8. Conclusion

Two Photon Physics studies at LEP have substantially improved (extended) the corresponding previous measurements. There are several measurements which have been performed for the first time in $\gamma\gamma$ collisions. Analysing the full LEP data sample will further contribute to this rich and important research field.

9. Acknowledgements

I would like to thank Stephan Narison for the lively atmosphere of the Conference and for the perfect organisation. I wish to thank my L3 colleagues of the two-photon physics, in particular, Maria Kienzle, Roger McNeil, Igor Vodopianov, and Maneesh Wadhwa, and also Richard Nisius and Stefan Soldner-Rembold from OPAL for interesting discussions, help and providing with compilation results.

REFERENCES

1. L3 Coll., M. Acciari *et al*, Phys. Lett. **B 408** (1997) 450.
2. OPAL Coll., K. Ackerstaff *et al*, Eur. Phys. J **C 14** (2000) 199.
3. L3 Coll., L3 note 2570; contrib. paper 622 of the 30th Intern. Conf. on High-Energy Physics, Osaka, Japan (2000).
4. A. Donnachie and P.V. Landshoff, Phys. Lett. **B 296** (1992) 227.
5. Review of Particle Physics, Eur. Phys. J. **C 3** (1998) 1.
6. A. Donnachie and P.V. Landshoff, hep-ph 9806344 (1998).
7. A. Donnachie, H.G. Dosch and M. Rueter, hep-ph 9810206 (1998).
8. R. Engel, Z. Phys. C **66**, 203 (1995);
R. Engel and J. Ranft, Phys. Rev. D **54**, 4246 (1996).
9. B. Badelek, J. Kwiecinski and A.M. Stasto , hep-ph 9903248 (1999).
P.Desgrolard, M. Giffon, E. Martynov and E. Predazzi, hep-ph 9811393 (1998).
10. R.M. Godbole and G. Pancheri, hep-ph 9903331 (1999);
A. Corsetti, R.M. Godbole and G. Pancheri, Phys. Lett. **B 435** (1998) 441.
11. L3 Coll., M. Acciari *et al.* Phys. Lett. **B 453** (1999) 83.
12. M. Drees, M. Krämer, J. Zunft and P.M. Zerwas, Phys. Lett. B **306**, 371 (1993).
13. ALEPH Coll., D. Buskulic *et al*, Phys. Lett. B **355**, 595 (1995); the ALEPH note 031, 2000.
14. L3 Coll., M. Acciarri *et al*, Phys. Lett. B **453**, 83 (1999); Phys. Lett. B **467**, 137 (1999); L3 note 2548, contrib. paper 584 to ICHEP2000, Osaka, Japan (2000).
15. L3 Coll., L3 note2565, contrib. paper 582 to ICHEP2000, Osaka, Japan (2000).
16. OPAL Coll., G. Abbiendi *et al*, CERN-EP/99-157, Eur. Phys. J. C accepted.
17. CDF Coll., F. Abe *et al*, Phys. Rev. Lett. **71**, 500,2396,2537 (1993); Phys. Rev. Lett. **75**, 1451 (1995);Phys. Rev. Lett. **79**, 572 (1997).
18. DØColl., S. Abachi *et al*, Phys. Rev. Lett. **74**, 3548 (1995).
19. H1 Coll. , C. Adloff *et al*, Phys. Lett. B **467**, 156 (1999).
20. ZEUS Coll. , O. Deppe *et al*, Proc. of PHOTON99, Nucl. Phys. B. (Proc. Suppl.), **82** 206-211, 2000.
21. J. Binnewies, B.A. Kniehl and G. Kramer, Phys. Rev. D**58** (1998) 014014; Phys. Rev. D**53** (1996) 6110.
22. S. Frixione, M. Krämer and E. Laenen, D* *Production in Two-Photon Collisions*, hep-ph/9908483, submitted to Nucl. Phys. (1999).
23. ALEPH Coll., D. Buskulic *et al*, Phys. Lett. B **458**, 152 (1999).
24. DELPHI Coll., P. Abreu *et al*, Z. Phys. C

69, 223 (1996); I. Tyapkin, Proc. of PHOTON97, p.26; Proc. of workshop on Photon Interactions and the Photon Structure, Lund, Sweden, p.59, (1998).
25. L3 Coll., M. Acciarri *et al*, Phys. Lett. B **436**, 403 (1998); Phys. Lett. B **447**, 147 (1999);
26. L3 Coll., M. Acciarri *et al*, Phys. Lett. B **483**, 373 (2000).
27. OPAL Coll., K. Ackerstaff *et al*, Z. Phys. C **74**, 33 (1997); Phys. Lett. B **411**, 387 (1997); Phys. Lett. B **412**, 225 (1997); G. Abbiendi *et al*, CERN-EP-2000-82, subm. to Eur. Phys. J C.
28. R. Nisius, Private communication.
29. PLUTO Coll., Ch. Berger *et al*, Phys. Lett. **B 142** (1984) 119.
30. ALEPH Coll., C.A. Brew, S. Cartwright, M. Lehto, Proc.of PHOTON97, p.21, (1997); DELPHI Coll., A. Zintchenko *et al*, Proc. of PHOTON99, Nucl. Phys. B. (Proc. Suppl.), **82** 43, 2000.
L3 Coll., M. Acciarri *et al*, Phys. Lett. B **438**, 363 (1998);
OPAL Coll., G. Abbiendi *et al*, Eur. Phys. J. C**11** (1999) 239.
31. CERN-EP-2000-109, subm. to Eur. Phys. J C.
32. R. Nisius, Phys. Rep. 332 (2000) 165.
33. E.A. Kuraev, L.N. Lipatov and V.S. Fadin, Sov. Phys. JETP **45** (1977) 199; Ya.Ya. Balitski and L.N. Lipatov, Sov. J. Nucl. Phys. **28** (1978) 822.
34. L3 Coll., M. Acciari *et al.* Phys. Lett. **B 453** (1999) 333; L3 note 2568, contrib. paper 587 to ICHEP2000,Osaka, Japan(2000).
35. S.J. Brodsky *et al*, Phys. Rev. **D 56** (1997) 6957;
J. Bartels *et al*, Phys. Lett. **B 389** (1996) 742; hep-ph/9710500.
36. V.M. Budnev *et al., Phys. Rep.* **C 15** (1975) 181. G.A. Schuler, *Comput. Phys. Commun.* **108** (1998) 279.
37. OPAL Coll., T. Ackerstaff *et al.*, Eur. Phys. J. C **6** (1999) 253; Eur. Phys. J. C **10** (1999) 547;
38. T. Kleinwort, G. Kramer, 1996 *Nucl. Phys.* B **477** 3; 1996 *Phys. Lett.* B **370** 141; M. Klasen, T. Kleinwort, G. Kramer, private communication.
39. L3 Coll., O. Adriani *et al*, Phys. Lett. B **286**, 403 (1992); M. Acciarri *et al*, Phys. Lett. B **363**, 118 (1995); Phys. Lett. B **413**, 147 (1997); Phys. Lett. B **418**, 399 (1998).
40. L3 Coll., L3 note 2594, contrib. paper 618 to ICHEP2000, Osaka, Japan(2000).
41. L3 Coll., L3 note 2589, contrib. paper 599 to ICHEP2000, Osaka, Japan(2000).
42. L3 Coll., L3 note 2557, contrib. paper 603 to ICHEP2000, Osaka, Japan(2000).
43. L3 Coll., L3 note 2564, contrib. paper 589 to ICHEP2000, Osaka, Japan(2000).
44. L3 Coll., M. Acciarri *et al*, Phys. Lett. B **461**, 155 (1999).
45. L3 Coll., M. Acciarri *et al*, Phys. Lett. B **453**, 73 (1999).
46. OPAL Coll., K. Ackerstaff *et al*, Phys. Lett. B **439**, 197 (1998).
47. DELPHI Coll., P. Abreu *et al*, Phys. Lett. B **441**, 479 (1998).
48. ALEPH Coll., D. Buskulic *et al*, Phys. Lett. B **472**, 189 (2000).
49. TPC/2γ Coll., D.A. Bauer *et al*, Phys. Lett. B **302**, 345 (1993).
50. CLEO Coll., J. Dominick *et al*, Phys. Rev. D **50**, 4265 (1994).
51. C. Michael, Nucl. Phys. **A 655** (1999) 12 and references therein.
52. BES Coll., J. Z. Bai *et al*, Phys. Rev. Lett.**76** (1996) 3502;
Mark III Coll., R. M. Baltrusaitis *et al*, Phys. Rev. Lett.**56** (1986) 107.
53. Crystal Ball Coll., D. Antreasyan *et al*, Phys. Rev.**D 36** (1987) 2633.
54. E835 Coll., M. Stancari, Proc. of PHOTON99, Nucl. Phys. B. (Proc. Suppl.), **82** 306, 2000.
55. E760 Coll., T.A. Armstrong *et al*, Phys. Rev. Lett. **70**, 2988 (1993);
56. T. Feldmann and P. Kroll, Phys. Lett. **B 413** (1997) 410.